Department of Electrical
and
Computer Systems Engineering

Technical Report
MECSE-1-2008

Paired Measurement Localization: A Robust Approach for Wireless Localization

M. Z. Rahman and L. Kleeman

MONASH
UNIVERSITY

Paired Measurement Localization: A Robust Approach for Wireless Localization

Mohammed Ziaur Rahman, and Lindsay Kleeman

***Abstract*—Location awareness remains the key for many potential future applications of distributed wireless ad-hoc sensor networks (WSNs). While location of a WSN node can be estimated by incorporating Global Positioning System (GPS) devices, it is not possible at present to embed GPS receivers in every node considering the cost and size of these devices as well as from optimization point of view. However, a small number of WSNs nodes called anchor nodes are able to resolve their location either through fixed deployment or using GPS receivers and thereby provide the reference framework for localization of other nodes. The measurement devices in individual nodes are often erroneous for tiny WSNs nodes and hence robustness is a major issue for localization. In this paper a theoretical localization framework in the presence of noise is postulated, which achieves accurate positioning compared to the existing theoretical and statistical estimation methods employing a theoretical minimum number of four anchor nodes. The paired measurement localization (PML) strategy is evaluated through simulations under various noise conditions and environmental modeling; and practically verified by a test-bed implementation with real motes. The results corroborate the improved positioning as well as robustness of PML for ad-hoc wireless sensor networks in presence of noise.**

I. Introduction

THE emergence of small hardware devices that possess limited computing, communications and sensing capabilities has been the core foundations for Wireless Sensor Networks (WSNs), with a diversity of application domains evolving from habitat monitoring and smart traffic systems through to surveillance and target tracking [11, 25].

A typical WSN comprises nodes having a low powered processor with a small amount of onboard memory, a wireless transceiver and some battery powered sensors. This means that certain inherent constraints on the networks design can be distilled including, *i*) limited processing capability, *ii*) limited communication range, *iii*) restricted battery lifetime, *iv*) coarse sensing potential and *v*) low reliability in supporting miniature nodes, *e.g.*, form-factor of the WSN devices.

For the purposes of efficient management and distributed collaboration of these tiny devices, some control nodes can be employed which have greater processing and communications capabilities, together with a more reliable power source.

Location awareness is vital for many WSN applications such as routing [20], and for achieving higher network security [18] and energy efficient node management [39] as well as many next generation location based services.

Positioning can be of two types such as relative positioning and absolute positioning. This paper focuses on absolute positioning where some WSN nodes know their positions either through manual deployment at a fixed location or using Global Positioning System (GPS) devices and designated as anchor nodes (also called seed nodes in [17]). The position of general nodes is to be determined either from the distance of the node from the anchor nodes (range estimation) or the angle of the node with the anchor nodes (bearing estimation). Beacon nodes are also sometimes used for this purpose, with in [19] they being differentiated from anchor nodes as generally requiring some fixed infrastructural deployment for localization [4, 26].

WSN localization is a very challenging task since as already alluded there are significant device constraints which impact upon the design objectives for any practical localization scheme. A generic set of design objectives therefore include [15, 19, 37]: *i*) independence from anchor node placement, *ii*) being supported by a low density of nodes, with a minimal relative density of anchor nodes, *iii*) robustness - tolerance to node failures and range errors, *iv*) energy efficiency - minimal computation, communication and support for sleep mode for maximizing battery lifetime, *v*) simple measurement hardware for both cost effectiveness and device size miniaturization, and *vi*) support for distributed algorithms, for true ad hoc network operation without any central coordination overhead.

With respect to design objective *v*), range-based techniques are far more suitable than bearing-based approaches as they mandate either little or no additional hardware requirement to support the small form-factor of WSN devices though it is more erroneous than bearing-based estimations. Hence range measurement based positioning is focused in this paper.

As Chintalapudi et al. [9] confirms, no single existing source localization algorithm currently fulfils all the above design objectives, with a review of available localization algorithms coming to the overall conclusion that acceptable performance cannot be satisfactorily achieved for all design objectives because of their conjectured fundamental limitation of ad-hoc localization systems using only range-based measurements. Langendoen and Reijers [19] further established that no algorithm performed best in all aspects so providing the motivation for this paper, which presents Paired Measurement Localization (PML) that fulfils the aforementioned design objectives under noisy conditions at a satisfactory level over others.

It will firstly be observed that under the precise condition of equidistant sensors, range measurement errors become insignificant for location estimation. Based upon the observation, an exact formulation of hyperbolic locus of the source node will be found under the assumption of equal noise presence

Dept. of Elec. & Comp. Systems Engg.
Monash University, Clayton, Melbourne, Australia.

for a pair of anchors. Solution of hyperbolic location is non-trivial and two methods will be presented for closed form solution under different conditions. Also, a refined and linear locus of the source node will be found for PML under specific measurement noises for a pair of nodes that provided another approach to PML localization. Simulation and experimental results corroborate both the effectiveness and robustness of the new PML algorithm.

The PML approach follows from theoretical improvement of the original noisy locus and also provides closed form solution. Hence, it is computationally highly efficient compared to other robust localization approaches which either employ an error refinement phase [21] or require very low measurement noise as a precondition of accurate operation [22]. Among range measurement techniques, *Received Signal Strength (RSS)* is the simplest approach as most radio communication devices come with built-in RSS indicator (RSSI) hardware, though this is also the most error prone range estimator. PML is both simulated and practically verified for RSS-based range measurements to highlight its potential for general WSNs localization. It is independent of node placement and simulated for randomly deployed node scenarios. The communication cost is minimized as it is able to work with as low as four independent or three pairs of anchors and hence supporting a low anchor node density concomitant with energy preservation. Therefore, PML is truly distributed as all nodes can compute their locations upon receipt of adjacent anchor range measurements without any central coordinating intervention.

The remainder of the paper is organized as follows: Section II provides a review of location estimation methods, while Section III presents the RSS based range measurement model and Section IV discusses error characteristics used for WSN as one of the main objective of this paper is to present localization under erroneous conditions. Section V provides the paired measurement based hyperbolic locus formulation which is the basis for PML localization. It also provides three alternative ways for PML solution incorporating the basic principle. The simulation and practical performance of PML approach is thoroughly examined in Section VI and VII. Section VIII provides some conclusions.

II. Review of Related Works

While WSNs localization is a relatively new research topic, localization per se in the signal processing discipline is well established, with there also being strong linkages in robotics for robot localization and tracking purposes. This section explores some relevant strategies that exhibit the potential to be practically applied in a WSNs context to satisfy the six design objectives delineated in Section I.

As mentioned previously, only range-based techniques are considered in this paper. These can be broadly classified into two categories - *geometric* and *topological* [9] approaches. The former performs lateration [19] for localization from range measurements of either three or more anchor nodes, while the latter exploits topological and neighbourhood node relationships for location estimation from the relative distances between each node and anchor nodes.

As the PML method is independent of how range estimation is performed, the various merits and demerits of the ranging methods are examined to provide generic context, with special emphasis being given to their suitability for WSN applications.

A. Geometric Localizations

Geometric approaches to localization are based on accurate distance measurement from anchor nodes that already know their positions. Triangulation is the basis of these techniques and is generally sub-divided into: *i*) lateration, where the range measurements are used from $n+1$ sensors for an n-dimensional location estimation; and *ii*) angulation which uses the angle of arrival (bearing) measurements combined with distance [24]. Bearing estimates necessitate sophisticated antenna arrays that are unsuitable for integration at the requisite form-factors and energy-levels of current WSN nodes [9], as well as rapidly exacerbating the localization accuracy under noisy measurements [31].

Range estimation can be achieved by any of the following metrics, *i*) *Time Of Flight* (TOF), *ii*) *Time Delay Of Arrival* (TDOA), or *iii*) *Received Signal Strength* (RSS). TOF is calculated from the start and receive times of a signal transmission. In the cricket location-support [26] system, this is achieved by an RF and ultrasound signal combination supported by beacon nodes that simultaneously transmit both an RF and ultrasound pulse, with the receiving node computing the TOF using the time difference of arrival between these two signals [9, 26]. This approach can achieve high accuracy (1-2% error of the transmission range) over a communication range of $3-6m$, which is significantly lower than the nominal radio range of sensor platforms such as mica motes, which has a range of tens of meters [9]. TOF requires a dense node deployment because the ultrasound signals usually only propagate up to $20-30feet$ [15]] and the relative anchor node density needs to be commensurately high. This approach also requires additional sensing and communications hardware for ultrasonic ranging.

The TDOA between two nodes is calculated from the individual time of arrival measurements and thus avoids the need for transmission of the originating time [32]. While it is suitable for broadband sources, the technique is very sensitive to clock synchronization between the nodes [8].

Amongst the various measurement approaches, RSS is the cheapest alternative in terms of hardware and communication requirements and is readily measured from the RSSI circuitry [24] in the receiver. Range estimation is then performed using a straightforward path-loss model for RF propagation through the space. There has been considerable interest recently in RSS-based localization because of its suitability to WSNs applications as exemplified by the SpotON [16], Calamari [37] and RADAR [2] systems. However, RSS-based range estimations are error-prone as the transmit power varies with battery power level and the receiver characteristics vary widely, even for similar nodes. Based on hardware variations, it has been shown that distance estimates between pairs of different transmit-ters/receivers can vary by as much as 300% [37]. Fine calibration [16, 37] is thus needed for effectual

RSS-based usage, while some researchers have postulated that this fundamental RSS limit may be insuperable [9]. Through the introduction of PML in this paper it is shown that it is possible to employ multi-hop localization from noisy RSS measurements to achieve much superior performance than original triangulation which is basis of most localization algorithms.

B. Topological Localization Methods

The three earliest approaches to topological localization were Convex Optimization [10], GPS-less [4] and GPS-free [6]. Convex Optimization finds the location by a set of convex constraints that require centralized high-end processing, while GPS-less estimates the location as the centroid of nearby anchor node positions, so mandating high density deployment of anchor nodes for moderate ac-curacy. GPS-free in contrast incurs high communication costs in order to establish a relative coordinate based location system. Another topological range-free method is the Approximate-Point-In-Triangle (APIT) [15] which applies a test as to whether a particular node lies inside a set of triangles formed by anchor nodes. The intersection of these triangles gives an improved estimate of the location, though this requires adequate anchor node density and sufficiently powerful computing resources to compute all the triangles. Hence none of these techniques satisfies the design objectives completely.

Langendoen and Reijers [19] selected three algorithms, *i*) Ad-Hoc Positioning [23]; *ii*) N-hop multilateration [30]; and *iii*) Robust Positioning by Savarese et al. [29]; as broadly fulfilling the design objectives, though no single algorithm has been shown to be the best in every aspect.

There are three common phases in these different topological localization methods, namely *i*) range estimation, *ii*) initial location estimation and *iii*) iterative refinement.

The ad-hoc positioning technique described in [23] is similar to distance-vector (DV) routing, where the distance (either hop or range) from an anchor node is flooded in a controlled manner throughout the network and each node maintains a minimum distance table to the anchor nodes. The DV approach can apply the hop count (DV-hop), or either the actual (DV-dist) or the Euclidean distance between neighbouring nodes. DV-hop and DV-dist are similar except that the former approximates the distance per hop and converts the hop distance to a range measurement. All DV-based algorithms however consistently overestimate the range, while the Euclidean approach provides superior accuracy, though often it underestimates the range, at the cost of greater communications and lower error resilience [19].

The iterative refinement phase can be achieved using classical Kalman Filter concepts [28], probabilistic refinement [12] and Maximum Likelihood (ML) estimation [33], although none of these approaches achieve significant improvements, particularly for erroneous RSS measurements. Statistical refinement techniques tend to be data driven and inherently inaccurate, with the lower error bound being given by the Cramer-Rao Lower Bound (CRLB) [8, 24] and unsuitable when only a small number of data samples (range measurements) are available.

A comprehensive analysis of location error sources, models and effects is provided in [34]. Certain algorithms which are aimed at improving localization performance do address erroneous measurements, such as those in [21, 22, 29]. In [29] for instance, a two-phase positioning system is introduced with the initial location estimation performed by Hop-TERRAIN, which is an algorithm similar to DV-hop. An iterative refinement process is subsequently applied in order to improve the position estimate. In [21], an iterative least square (ILS) approximation is introduced for gradual error refinement, so both Hop-TERRAIN and ILS are specializations of the iterative refinement step of [19]. In [22], the localization problem has been solved using a 2-D graph realization approach similar to the Euclidean distance measurement of [23] with the elimination of ambiguous localization caused by graph flips being attained using robust quadrilaterals. The localization error is minimized at the cost of a higher node degree, which implies increased anchor node density and poorer localization due to its inability to manage ambiguous circumstances.

In summarizing, range-based localization techniques inevitably incur measurement errors for WSN applications, so noise cancellation is a major focus of this paper. In the next section an RSS-based range measurement model is examined because it is the most expedient metric for localization.

III. RSS Measurement Model

Received signal strength in an idealistic physical environment is usually represented by the following formula:

$$\textit{RSS} = \textit{Sending Power} - \textit{Path Loss} + \textit{Fading} \tag{1}$$

where the path loss describes the large-scale signal attenuation while traveling through a medium and fading represent small-scale signal variations caused by multipath propagation, relative movement among receiver and surrounding objects, and signal transmission bandwidth.

A. Free Space Path Loss Model

This model gives the RSS signal attenuation for both transmitters and receivers that have an unobstructed line-of-sight (LOS) path between them. The signal strength still reduces by some exponent of distance, with the Friis free space equation for the attenuated received power under the free space propagation model being expressed as [27]:

$$P_r = \frac{P_t G_t G_r \lambda^2}{(4\pi)^2 d^2 L} \tag{2}$$

P_r is the received signal strength (*i.e.* power), P_t and G_t are the transmitted power and antenna gain respectively, G_r is the receiver antenna gain, d is the distance between the receiver and transmitter antennae, L is the system loss factor ($L \geq 1$) and λ is the wavelength in meters.

The Friis model predicts P_r for signals that in addition to LOS conditions also fulfil the far-field distance (d_f) or Fraunhofer region from the transmitting antenna implying the receiver distance is much larger than both the signal wavelength and transmitter antenna linear dimension. Clearly

(2) is undefined when $d = 0$, so assuming a Fraunhofer region and measuring the signal strength P_0 at a reference distance d_0, the signal strength at any distance can be found from:

$$P_r = P_0 \left(\frac{d_0}{d}\right)^2, \quad d \geq d_0 \geq d_f \tag{3}$$

The Friis model is effective for the ideal propagation scenario though a more pragmatic model is mandated for real environments, such as that presented in the following section.

B. Log-Distance Path Loss Model

This exploits the basic tenet of free space path loss that signal strength decreases with a power of distance, but rather than following the square of distance attenuation it employs an environmental path loss exponent n for modeling different kind of medium as shown in the following equation.

$$\bar{P_r} \propto \left(\frac{d_0}{d}\right)^n \bar{P_r}(dBm) = \bar{P_0}(dBm) + 10n \log\left(\frac{d_0}{d}\right) \tag{4}$$

The bars in (4) indicate the ensemble average over all possible values for d, while n varies between 2 to 6 depending upon the environmental conditions covering free-space through to very dense urban environments where propagation is severely affected by buildings.

In the following section a short discussion on error characteristics is presented to assist understanding of the different error sources and noise characteristics together with their potential impact upon PML.

IV. WSNs Error Characteristics and Modeling

Earlier presented signal propagation based range estimation models are mostly idealistic and isotropic assuming signal attenuates equally at different directions. However, the noise presence in reality is anisoptropic and variable with time and direction. Radio propagation is reported to be irregular on different directions [38]. In this section at first possible error sources are depicted. Subsequently practical path loss modeling by incorporation of statistical variation and Radio Irregularity Model (RIM) [38] is presented.

A. Error Sources

In [34] five major sources of error were identified that impact upon WSNs localization performance, namely:

1) Measurement
2) Finite precision
3) Objective function related
4) Intractable optimization tasks
5) Localized algorithms

Measurement errors arise due to limitations in the sensing technology, phenomena instability and environmental noise. Of particular importance in this regard, is receiver calibration as their characteristics can vary significantly, with one approach to minimizing this error source being dynamic calibration. The second error is omnipresent in all computing systems, while the third and fourth errors are caused by optimization issues, which are both problem and model specific. The final error is as a result of either spatial or proximity collaboration of nodes being used in the WSN localization.

The log-distance path loss model is now modified for consideration of error sources in the measurement as follows.

B. Practical Log-Distance Path Loss Model

The ability to appropriately model an error source can improve the overall performance of an algorithm that uses the model and assists as well in understanding the challenges in a more quantitative manner. This paper focuses specifically upon RSS measurements in its robustness evaluation because it is both the most convenient and error-prone metric for WSNs localization.

The main error source in RSS based range estimations is path loss, which is inversely proportional to the distance raised to some path loss exponent. A simplistic model that addresses only path loss will fail as highlighted in [32], since multi-path fading and shadowing also contribute significantly towards RSS range errors. These errors are specially prominent in urban environs due to reflection, scattering and diffraction from surrounding objects and buildings. It was reported in [32] that placing a node $1.5m$ above the ground triples the transmission over a ground node placement, under the same line-of-sight conditions.

The decibel (dB) error distribution for RSS is modelled as zero-mean Gaussian and is given by:

$$10n \log\left(\frac{\tilde{d}}{d_0}\right) - 10n \log\left(\frac{d}{d_0}\right) = X_\sigma \tag{5}$$

where d is the actual range, $\tilde{d}$ is the measured range between the transmitter and receiver, X_σ is the zero-mean Gaussian random variable with standard deviation σ and n is the path loss exponent. d_0 represents an arbitrarily close reference distance to the transmitter where the original transmitted signal is available to the receiver without any path loss. From (5), the RSS error can thus be formulated as follows:

$$RSS_{ERR}(d) = \tilde{d} - d = d\left(10^{\frac{X_\sigma}{10n}} - 1\right) \tag{6}$$

Variations in the transmitter and receiver characteristics due to manufacturing non-uniformities are another source of error and require calibration. However, due to the scale of a WSN, it is not always possible to calibrate individual nodes, so in the Calamari system [37] for example, *macro-calibration is used*. This is a dynamic calibrating method that is implemented by a generalized parameter estimation approach to error minimization, though it is not suitable for devices that exhibit different characteristics in different frequency bands.

C. Radio Irregularity Model

The radio irregularity model is devised for consideration of anisotropic propagation through the communication medium by the adjustment of path loss component as follows:

$$RSS = Sending\ Power - RIM\ Adjusted\ Path\ Loss + Fading \tag{7}$$

where *RIM Adjusted Path Loss = Path Loss* $\times K_i$, K_i representing the path loss adjustment coefficient for the i^{th} degree of the propagation and calculated randomly according to the Weibull distribution which fits well with practical variation of RSS [38] in different directions.

The next section presents the new PML strategy for range-based measurements in WSNs under erroneous range estimations. To our knowledge this is a unique approach to WSNs localization, to embed error cancellation within the mathematical formulation itself to achieve superior localization performance. The analytical formulation avoids any iterative refinement, which is computationally expensive and requires range estimation with the ensuing communications overhead from as many devices as possible in order to achieve satisfactory performance. In direct contrast, PML mandates a theoretical limit of four or three pairs of non collinear anchor node for localization and hence minimizes communications overhead significantly.

V. Localization in the Presence of Noise

Initially the ideal case is considered where noise effects are simplified by assuming equal noise presence and equidistant anchors from the source. An exact formulation is then derived for the *Locus Of Position* (LOP) of source node given a pair of anchors. The formulation is non-linear and two closed form solutions are presented next before introducing another approach that works by the refinement of the paired LOPs. For WSNs localization, it is also assumed that the surface is planar and all methods are two dimensional (2-D), though the proposed theory is sufficiently generic to be easily extended to three dimensions.

In the ideal scenario where no noise is present, it is feasible to calculate the exact node location using only three range measurements through triangulation [5]. Two range measurements can result in two solutions corresponding to the intersection of two circular LOPs. The third measurement resolves this ambiguity. This approach will now be augmented for location estimation in the presence of noise using the following analysis.

Observation 1: Assuming there is a node with range measurements from two anchor nodes that are equal and have equal error components, it is shown below that the locus of positions for that node (as the error components vary) is a straight line whose equation is independent of range measurements.

The 2-D source localization problem with three sensor nodes is shown in Figure 1(a).

The circles surrounding anchor nodes $\mathbf{p_1}\,(x_1, y_1)\,, \mathbf{p_2}\,(x_2, y_2)$ and $\mathbf{p_3}\,(x_3, y_3)$ denote the LOPs obtained from the individual range measurements for each node. Ideally, the LOPs surrounding anchor i is given by,

$$r_i^2 = \|\mathbf{p}_i - \rho\|^2 = \left((x - x_i)^2 + (y - y_i)^2\right) \tag{8}$$

In ideal noise-free conditions, any two such circular LOPs can be equated to simplify to a linear form representing a straight

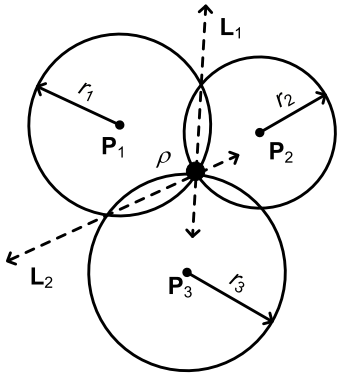

(a) Ideal 2-D triangulation scenario where linear form LOPs are found from the corresponding two circular LOPs [5].

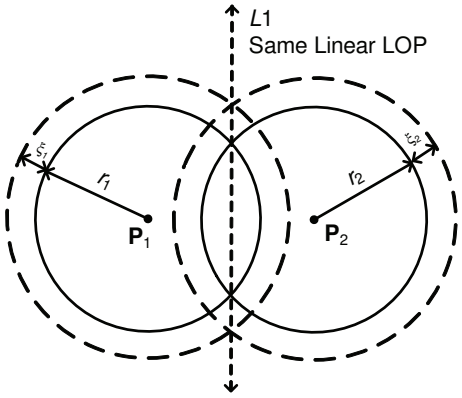

(b) LOP from equidistant sources in presense of equal noise.

Fig. 1: Depiction of observation 1.

line passing through two intersecting points of the circular LOPs. This line does not represent the actual locus of the source node as it will be clarified later. However, following [5] this line is refered as *Linear Form LOP* in the subsequent discussions. In figure 1, L_1 and L_2 are determined from the circular LOPs corresponding to anchor node pairs $(\mathbf{p_1}, \mathbf{p_2})$ and $(\mathbf{p_1}, \mathbf{p_3})$ respectively, with the intersection point (x, y) of L_1 and L_2 denoting the actual location of the source node.

Assume now that due to noise, the range readings for $\mathbf{p_1}$ $(x_1,\ y_1)$, $\mathbf{p_2}$ $(x_2,\ y_2)$ and $\mathbf{p_3}\,(x_3, y_3)$ are corrupted to give respective LOPs of radii $\tilde{r}_1 = r_1 + \xi_1$, $\tilde{r}_2 = r_2 + \xi_2$ and $\tilde{r}_3 = r_3 + \xi_3$, where $\tilde{r}_i$, r_i represent the observed and actual distance between the i^{th} anchor node and source node respectively and ξ_i is the measurement noise at anchor node i. The circular LOP can then be expressed as:

$$(r_i + \xi_i)^2 = \|\mathbf{p}_i - \rho\|^2 \tag{9}$$

where $\rho = (x, y)$ is the node position to be determined.

Equating the circular LOPs for $\mathbf{p}_1$ and $\mathbf{p}_2$ using (9), L_1 becomes:

$$\begin{aligned} &(x_2 - x_1)\, x + (y_2 - y_1)\, y = \\ &\tfrac{1}{2}\left(\|\mathbf{p}_2\|^2 - \|\mathbf{p}_1\|^2 + (r_1 + \xi_1)^2 - (r_2 + \xi_2)^2\right) \end{aligned} \tag{10}$$

where the right hand side becomes independent of range parameters, *i.e.*, measurement values $\tilde{r}_1$ and $\tilde{r}_2$ whenever $\tilde{r}_1 = \tilde{r}_2 \Rightarrow r_1 + \xi_1 = r_2 + \xi_2$. One particular case is equidistant anchor nodes and equal noise presence when the above condition is fulfilled.

The importance of this observation lies in the fact that it eliminates the signal energy dependent parameters under assumed conditions completely, which possess noisy characteristics and are also both device and environmentally dependent.

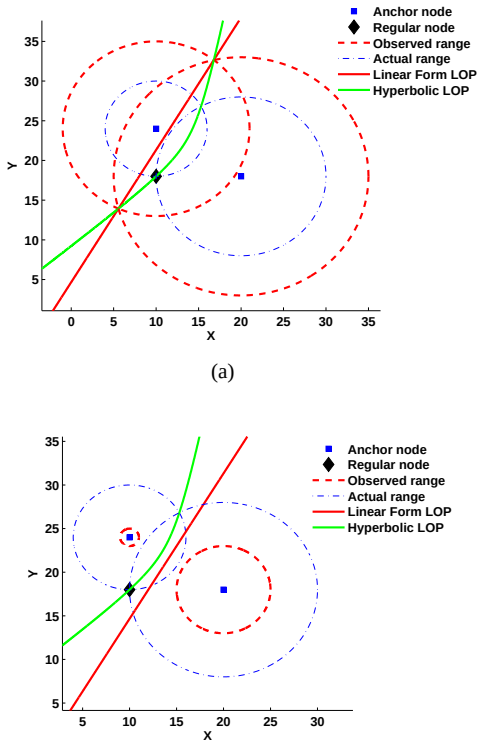

(a)

(b)

Fig. 2: The hyperbolic and linear form LOP of a regular node from range estimates by a pair of anchors under equal noise assumption. (a) The general case when two observed circular LOPs physically intersect. (b) The case when circular LOPs do not intersect due to noise and underestimation of the ranges.

Based upon the above observation and assuming only the equal noise presence, it is useful to explore paired measurements rather than individual ranges to mitigate the effect of noise. As the difference of the range estimates equate to actual difference for equal noise presence (*e.g.*, $\tilde{r}_2 - \tilde{r}_1 = r_2 - r_1$), the LOP for the target node is found by the locus of positions maintaining constant difference from the pair of anchors. Hence, the hyperbolic LOP of the target node can be found independent of the noise parameters as shown in figure 2 and formulated below:

$$\sqrt{(x-x_2)^2+(y-y_2)^2} - \sqrt{(x-x_1)^2+(y-y_1)^2} = (\tilde{r}_2 - \tilde{r}_1) \quad (11)$$

After algebraic manipulations, it takes the general hyperbolic form as follows for $\mathbf{p}_1 = (0,0), \mathbf{p}_2 = (a,0)$, and $r_1 - r_2 = c$.

$$\left(x - \frac{a}{2}\right)^2 - \frac{y^2}{\left(\frac{a^2}{c^2} - 1\right)} = \frac{c^2}{4} \quad (12)$$

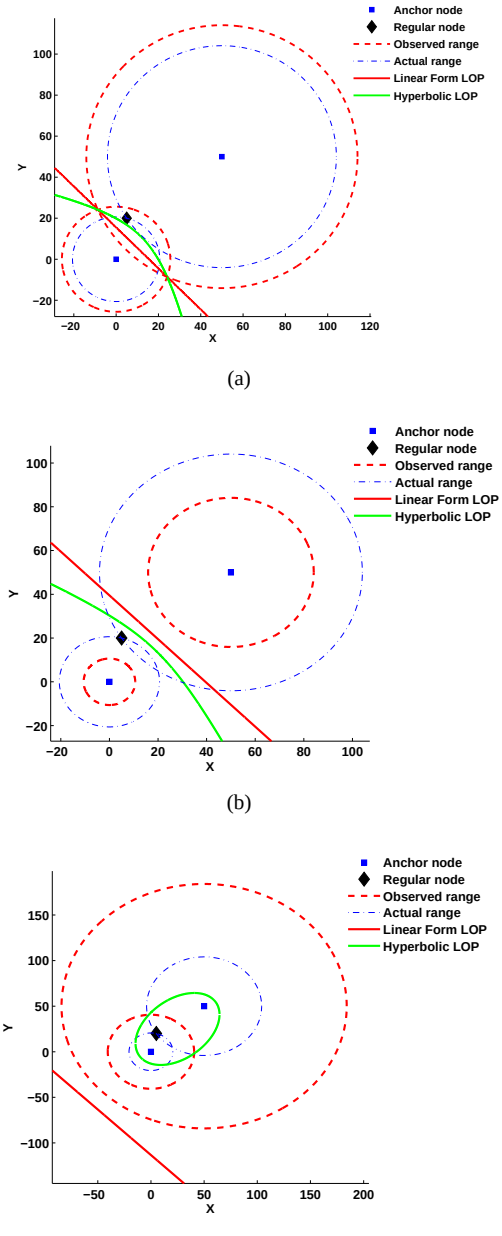

(a)

(b)

(c)

Fig. 3: The hyperbolic and linear form LOPs for unequal noise presence. (a) The general case when two observed circular LOPs physically intersect. (b) The case when observed circular LOPs do not intersect due to underestimation of the ranges. (c) The case when observed circular LOPs do not intersect but overlap completely due to overestimation of the ranges .

The hyperbolic LOP represents the exact LOP for a pair of anchors under the equal noise assumption. The linear form LOP does not truly represent the locus of source node under noise unless both ranges to anchor nodes are equal despite its use in [5] as clarified in figure 2. Two possible cases could

arise due to equal noise presence: *a*) the circular ranges have physical intersection and *b*) the circular ranges do not have any physical intersection. In both cases, hyperbolic LOP is able to represent the original target position whereas linear form LOP deviates from target position significantly. As establishing the LOP is the first step in localization, any error present at this step could aggravate the result significantly and hence finding a LOP closer to the original source node is fundamental to achieving high accuracy localization.

It is also crucial to compare the hyperbolic and linear form LOPs for unequal noise components in individual measurements as in reality this assumption can be void. In these general situations three possible cases could arise. *a*) the observed circular ranges have physical intersection; *b*) the observed circular ranges do not have any common intersection region; and *c*) One of the observed circular ranges overlap completely within the other circular region.

These three cases are shown in figure 3 where figure 3(a), (b) shows the hyperbolic and linear form LOPs for noise ratio $\left(\frac{\xi_1}{\xi_2}\right)$ of 2 while 3(c) shows the LOPs for noise ratio of 4. Figure 3(c) also shows that for completely overlapped ranges the hyperbolic formulation turns into elliptic formulation as the coefficient of y^2 in 12 changes sign as the range difference becomes greater than distance between the anchors ($c > a$). It is evident from the figures that in all the three cases of unequal noise presence, hyperbolic formulation is better suited than linear form and the impact of noise is less detrimental on hyperbolic LOPs than it is on linear form LOPs.

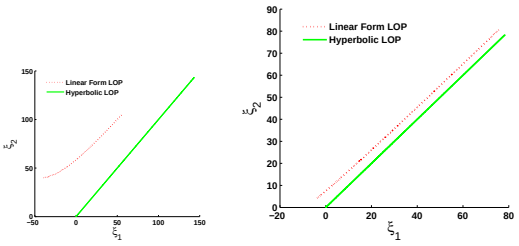

(a) (b)

Fig. 4: Comparison of equal noise effect on hyperbolic and linear form LOPs. Anchor nodes are placed at (0, 0) and (0, 50) while source node is placed at (a) (0, 27) and (b) (0, 45).

A 2-D plot for noise components ξ_1, ξ_2 is shown in figure 4(a), (b). The hyperbolic LOP maintains $\xi_1 = \xi_2$ throughout its path and hence, the noise plot is linear passing through the origin. The noise relationship is non-linear for linear form LOP and as the range difference increases, the linear form LOP performs worse as its distance from actual source locus is increased further.

Solving the nonlinear hyperbolic equations is difficult. Moreover, existing hyperbolic localization methods proceed by linearizing the system of equations using either Taylor-series approximation [13, 36] or by linearizing with another additional variable [7, 14, 35]. However, while linearizing works well for existing approaches it is not readily adaptable for proposed paired approach as linearizing is indeed pairing with an arbitrarily chosen hyperbolic LOP. The assumption of equal noise cannot be held for any arbitrary selection of pairs and hence alternate ways to solve such LOPs for paired measurement is now formulated.

A. PML with Single Reference Anchor

Chan and Ho [7] provided closed form least square solution for non-linear hyperbolic LOPs by linearizing with reference to a single measurement node. Analogous to their approach a closed form solution is found for PML using pairs having a common reference anchor in them. The solution is simpler than [7]'s approach as the effect of noise is considered early in the paired measurements formulations.

Let $r_{\widehat{ij}}$ represent the difference in the observed ranges for anchor pairs (i, j). In case of equal noise presence it follows:

$$\begin{gathered} \tilde{r}_{\widehat{ij}} = r_{\widehat{ij}} = r_i - r_j \\ \text{After squaring and rearranging,} \\ r_i^2 = r_{\widehat{ij}}^2 + 2r_{\widehat{ij}} r_j + r_j^2 \end{gathered} \tag{13}$$

Hence, using the above the actual circular LOP can be transformed as follows:

$$(x - x_i)^2 + (y - y_i)^2 = (r_{\widehat{ij}})^2 + 2r_{\widehat{ij}} r_j + (r_j)^2 \tag{14}$$

Using (14) for pairs $(\mathbf{p}_i, \mathbf{p}_j) = (\mathbf{p}_k, \mathbf{p}_1)$ and $(\mathbf{p}_l, \mathbf{p}_1)$ and subtracting the second from the first,

$$\begin{aligned} -(x_k - x_l)x - (y_k - y_l)y - (r_{\widehat{k1}} - r_{\widehat{l1}})r_1 \\ = \tfrac{1}{2}\left((r_{\widehat{k1}})^2 - (r_{\widehat{l1}})^2 - \|\mathbf{p}_k\|^2 + \|\mathbf{p}_l\|^2\right) \end{aligned} \tag{15}$$

where $\|\mathbf{p}_k\|^2 = (x_k^2 + y_k^2)$. The above formulation represents a set of linear equations with unknowns x, y and r_1 for all combination of two pair of anchors having node 1 in common. Let $x_{\widehat{ij}}, y_{\widehat{ij}}$ represent the difference $x_i - x_j, y_i - y_j$ respectively, $\mathbb{C}_i$ represent the i^{th} combination and m represent the total number of combinations with $\mathbb{C}_i = \{(\mathbf{p}_{k_i}, \mathbf{p}_1), (\mathbf{p}_{l_i}, \mathbf{p}_1)\}$. The system of linear equations for these m combinations can be concisely written as follows:

$$\mathbf{AX} = \mathbf{B} \tag{16}$$

where,

$$\mathbf{A} = -\begin{bmatrix} x_{\widehat{k_1 l_1}} & y_{\widehat{k_1 l_1}} & -\left(r_{\widehat{k_1 1}} - r_{\widehat{l_1 1}}\right) \\ x_{\widehat{k_2 l_2}} & y_{\widehat{k_2 l_2}} & -\left(r_{\widehat{k_2 1}} - r_{\widehat{l_2 1}}\right) \\ . & . & . \\ x_{\widehat{k_m l_m}} & y_{\widehat{k_m l_m}} & -\left(r_{\widehat{k_m 1}} - r_{\widehat{l_m 1}}\right) \end{bmatrix},$$

$$\mathbf{X} = \begin{bmatrix} x \\ y \\ r_1 \end{bmatrix}, \mathbf{B} = \frac{1}{2}\begin{bmatrix} (r_{\widehat{k_1 1}})^2 - (r_{\widehat{l_1 1}})^2 - \|\mathbf{p}_{k_1}\|^2 + \|\mathbf{p}_{l_1}\|^2 \\ (r_{\widehat{k_2 1}})^2 - (r_{\widehat{l_2 1}})^2 - \|\mathbf{p}_{k_2}\|^2 + \|\mathbf{p}_{l_2}\|^2 \\ . \\ (r_{\widehat{k_m 1}})^2 - (r_{\widehat{l_m 1}})^2 - \|\mathbf{p}_{k_m}\|^2 + \|\mathbf{p}_{l_m}\|^2 \end{bmatrix}$$

For $m \geq 3$, the system of equations can be solved. However, r_1 is related to x, y by (8). For pairing and equivalence of $\tilde{r}_i -$

$\tilde{r}_1 = r_i - r_1$, observed ranges are always used in the equations and thus the system of equations are essentially independent of relationship between (x, y) and r_1. This is also verified by iterative refinement of r_1 where $\tilde{r}_1$ is modified by obtained r_1 in successive runs. The results show no difference in position estimates (x, y) for successive iterations.

The equal noise assumption cannot be applied to any arbitrary selection of pairs while it is quite reasonable for anchors observing near equal ranges to have equal noise components. The selection of pairs with near equal ranges from a single reference anchor, may not be feasible for low anchor densities. This is the motivation for the next solution approach.

B. PML with Equal Range Noise

Let $\mathbb{P}_i = \left(\mathbf{p}_1^i, \mathbf{p}_2^i\right)$ be an arbitrary node pair, where $\mathbf{p}_1^i = \left(x_1^i, y_1^i\right)$ and $\mathbf{p}_2^i = \left(x_2^i, y_2^i\right)$ represent anchor positions of the i^{th} pair. Using (10) and assuming equal and constant noise presence for a particular instance *i.e.* $\xi_1 = \xi_2 = \xi$, the equation for LOP L_i using anchor pair $\mathbb{P}_i$ is found from (10) as follows:

$$\begin{aligned}&\left(x_2^i - x_1^i\right) x + \left(y_2^i - y_1^i\right) y = \\ &\tfrac{1}{2}\left(\|\mathbf{p}_2^i\|^2 - \|\mathbf{p}_1^i\|^2 + \left(r_1^i\right)^2 - \left(r_2^i\right)^2 + 2\xi\left(r_1^i - r_2^i\right)\right)\end{aligned} \tag{17}$$

The equation becomes linear in terms of x, y and ξ if the noise is represented by a single parameter ξ for all pairs. This is obviously a simplification but it has the advantage of being able to work with anchor nodes as few as three for selection of three pairs from them. Thus, this method only extends the equal noise assumption from two to three nodes for providing a closed-form solution and hence is a competitive approach over others in many instances.

C. PML with Refinement of the Locus of Positions

The assumption of equal range noise is a simplification and while it will be shown later in the results section that it is superior to triangulation most of the cases, occassionally it performs worse. In search for a localization approach that can give consistently better estimates than basic triangulation, a locus refinement approach is now presented for arbitrarily placed anchors.

A refined and better approximation to linear form LOP is found from two imprecise linear form LOPs assuming equal noise presence in each pair and for specific instance of measurement as follows.

Figure 5 shows the ideal scenario where the position of the node to be determined, ρ, and the two respective linear form LOPs O_i and O_j are obtained from any two arbitrary anchor node pairs $\mathbb{P}_i$ and $\mathbb{P}_j$.

The equation for L_i, L_j can be found using (17). For specific measurement instance ξ is constant and L_i, L_j vary from the ideal noise free LOPs O_i, O_j by the extra constant terms of $2\xi\left(r_1^i - r_2^i\right)$, $2\xi\left(r_1^j - r_2^j\right)$ respectively. Crucially their slopes remain unchanged (Left hand side of (17)), and these are shown by the solid lines L_i, L_j parallel to O_i and O_j in Figure 5. For non collinear anchor node pairs, L_i and L_j will have a physical intersection point $\mathbf{I}_{ij} = (x_{ij}, y_{ij})$.

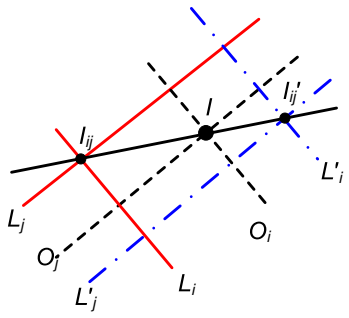

Fig. 5: Estimating the locus of node position under noisy measurement conditions.

Another line $L_i^{'}$ parallel to L_i can be found as follows by modifying the term $2\xi\left(r_1^i - r_2^i\right)$ with $-k\left(r_1^i - r_2^i\right)$, where k is an arbitrary positive constant.

$$\begin{aligned}&\left(x_2^i - x_1^i\right) x + \left(y_2^i - y_1^i\right) y = \\ &\tfrac{1}{2}\left(\|\mathbf{p}_2^i\|^2 - \|\mathbf{p}_1^i\|^2 + \left(r_1^i\right)^2 - \left(r_2^i\right)^2 - k\left(r_1^i - r_2^i\right)\right)\end{aligned} \tag{18}$$

The original LOP O_i will then pass between lines $L_i^{'}$ and L_i as the constants have opposite signs. A similar argument applies to $L_j^{'}$ so that the parallelogram bounded by the lines O_i, L_i, O_j, L_j will have an aspect ratio $AR = \left(\frac{r_1^i - r_2^i}{r_1^j - r_2^j}\right)$ as L_i is $2\xi\left(r_1^i - r_2^i\right)$ distance away from O_i and L_j is $2\xi\left(r_1^j - r_2^j\right)$ distance away from O_j as evident from the difference in the constant terms in (17). The AR of the parallelogram bounded by the lines O_i, $L_i^{'}$, O_j, $L_j^{'}$ will have exactly the same aspect ratio so indicating $\mathbf{I}_{ij}$, $\mathbf{I}_{ij}^{'}$ and $\mathbf{I}$ to be collinear points, where $\mathbf{I}_{ij}^{'}$ denotes the intersection point of lines $L_i^{'}$ and $L_j^{'}$.

Hence, the equation of the actual LOP $\mathbf{I}_{ij}\mathbf{I}_{ij}^{'}$ passing through $\mathbf{I}$ is found from the two intersection points $\mathbf{I}_{ij}$ and $\mathbf{I}_{ij}^{'}$ which are available from equations (17) and (18) and analogous equations for LOP L_j and $L_j^{'}$.

LOPs obtained from all possible combination of pairs $(\mathbb{P}_i, \mathbb{P}_j)$ from three pairs $(\mathbb{P}_1, \mathbb{P}_2, \mathbb{P}_3)$ can be written in the concise form as follows:

$$\mathbf{HX} = \mathbf{C} \tag{19}$$

where,

$$\mathbf{H} = \begin{bmatrix} y_{12} - y_{12}^{'} & -\left(x_{12} - x_{12}^{'}\right) \\ y_{13} - y_{13}^{'} & -\left(x_{13} - x_{13}^{'}\right) \\ y_{23} - y_{23}^{'} & -\left(x_{23} - x_{23}^{'}\right) \end{bmatrix}, \quad \mathbf{X} = \begin{bmatrix} x \\ y \end{bmatrix},$$

$$\mathbf{C} = \begin{bmatrix} x_{12}^{'}\left(y_{12} - y_{12}^{'}\right) - y_{12}^{'}\left(x_{12} - x_{12}^{'}\right) \\ x_{13}^{'}\left(y_{13} - y_{13}^{'}\right) - y_{13}^{'}\left(x_{13} - x_{13}^{'}\right) \\ x_{23}^{'}\left(y_{23} - y_{23}^{'}\right) - y_{23}^{'}\left(x_{23} - x_{23}^{'}\right) \end{bmatrix}$$

The solution of (19) gives the least square estimate of all possible LOPs using observation 1 and above mentioned LOP refinement procedure.

The locus refinement formulation assumes noise to be present in the formulae. However, if the noise is absent the two points $\mathbf{I}_{ij}$ and $\mathbf{I}_{ij}^{'}$ would be very close and during the calculation process whenever pairs having distance $< 3m$ are observed the estimated location is found as the mean of these two.

The linear form LOP obtained from each sensor pair must be linearly independent so they do not represent either the same or a parallel linear LOP. Such sensor pairs are referred to as mutually independent, so a key objective is to identify such sensor pairs, where each sensor receives equal signal strength. PML may be intuitively viewed as localization exploiting bearing measurements, as LOPs effectively denote a directional line. It is known that angular measurements are consistently more accurate compared to TOF range measurements and in [9] a combination of range and angular measurement has been shown to achieve better localization results, providing a valuable insight as to why the LOP refinement furnishes better location estimation. This will be corroborated by the simulation and practical results in Section VI and VII.

D. Selection of Anchor Pairs for PML

It is apparent from observation 1 that the existence of a pair of sensors having equal distance from the source node is vital for location estimation, with this prerequisite being relaxed and generalized by LOP refinement approach. Observation 1 highlights the significance of pairing the anchor nodes for better noise cancellation and a better selection process can result in considerable improvement. With practical range estimations there is no explicit way to determine the best possible pairs following the observation. However, the range estimation ratios can be used as a rough measure of adhere to observation 1 which is the basis for the following empirically defined ranking criteria. The ranking criteria also considers the closeness of the anchors. If the two anchors are too close to each other they might have the best range estimation ratio while effectively they are like two anchors placed at the same place and hence providing no additional redundancy to help localization. Utilizing, the above mentioned two principles the following empirical ranking criteria is introduced.

$$\Re = \frac{\tilde{r}_1}{\tilde{r}_2}\left(\frac{1}{\|\mathbf{p}_1\mathbf{p}_2\|}\right) \tag{20}$$

where $\tilde{r}_1$ and $\tilde{r}_2$ are the observed range estimates for anchor node pair ($\mathbf{p}_1$, $\mathbf{p}_2$) such that $\tilde{r}_1 \geq \tilde{r}_2$ and $\|\mathbf{p}_1\mathbf{p}_2\|$ is the Euclidean distance between two anchor nodes. The pairs having lower rankings ($\Re$) are chosen (*Algorithm* 1) following the ranking criteria. The complete node selection algorithm is given as follows.

Algorithm 1 searches all the available anchor nodes of a particular node so its computational complexity is O(*available anchor node*^{2}) if an exhaustive search is applied. Typically nearest anchors would have strongest signals experiencing least noise and interference. Hence, the nearest 6 anchors are chosen from available anchors and then pairs of anchors are chosen using Algorithm 1. This selection process can be run on-demand only when anchor positions are either changed or anticipated and given the relative small percentage of anchor nodes, this will incur negligible cost.

Algorithm 1 Anchor Node Selection

for all pair of neighboring anchor nodes **do**
  Update average neighbor range ($\bar{r}$) for calculating the current average range estimate;
  Calculate rank ($\Re$) for the pair $(\mathbf{p}_i, \mathbf{p}_j)$;
  if $(\mathbf{p}_i, \mathbf{p}_j)$ is collinear with any previous selected pair **then**
    Replace the previous collinear pair with current pair
  else
    if Number of selected pair $<$ Required number of pairs **then**
      Add current pair to selected pairs
    else
      Replace the worst ranking selected pair with current pair
    end if
  end if
end for

TABLE I: Simulation Parameters

Parameter	Range of Values
Radio Frequency	$1dBm$
Transmit Signal Strength	$1dBm$
Receive Signal Gain	0
Reception Sensitivity	$91dBm$
Reception Threshold	$81dBm$
Radio Placement Height	$1.5m$
Ambient Noise	$0mW$
Temperature Factor	0
Temperature	$290\,\mathrm{deg}$
SNR Threshold	10.0
Path Loss Exponent (n)	$2.0 - 2.2$
Ricean Fading parameter (K)	$6dB$
Anchor Percentage (p)	$5 - 15$
Field Size	$500m \times 500m$
Number of nodes	$200 - 1000$

Finally, as the new PML method itself is an analytical approach, the order of computational complexity is $O(1)$ once node selection has been completed. The communications overhead including bandwidth and transmission costs for node location estimation are minimized as only three pairs of anchor nodes need to transmit the range estimates localization of a node. The simulation performance of PML will now be analyzed.

VI. Simulations and Modeling Results

Java-based simulation tool Java in Simulation Time (JiST) developed by Barr et al. [3] is used for discrete event simulation of WSNs as it provides a transparent, efficient and standard simulation framework. Using JiST, a *Scalable Wireless Ad Hoc Network Simulator* (SWANS) has also been developed which is highly scalable and memory efficient and suitable for WSNs simulation scenarios having a very large number of nodes. SWANS has been shown to scale for up to

1 million nodes while popular *ns2* network simulator supports only a few hundred nodes and GloMoSim (another popular ad-hoc wireless simulation tool), supports up to 10000 nodes.

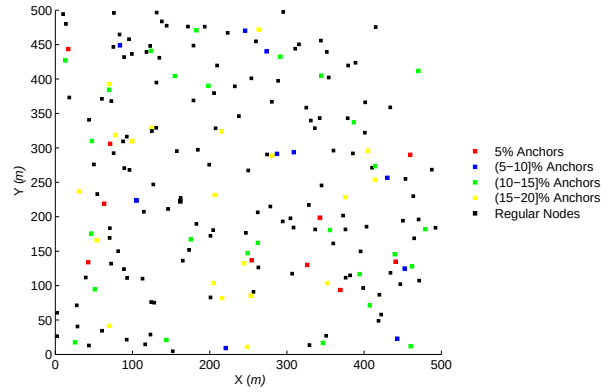

(a)

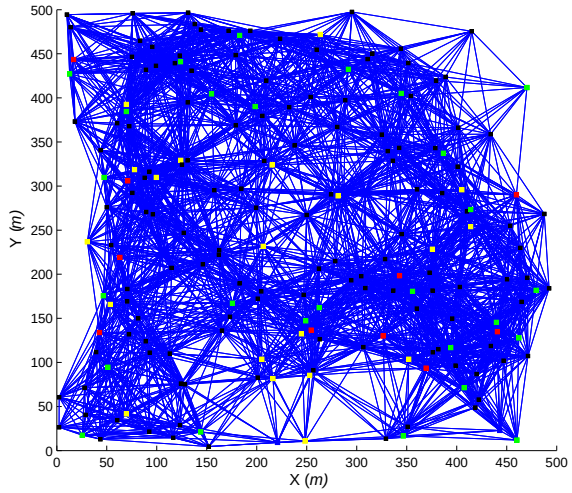

(b)

Fig. 6: A WSNs deployment scenario at a $500m \times 500m$ field: (a) shows the node distribution with anchors and regular nodes marked in different colors for different percentages; and, (b) shows the nodes as they are interconnected with each other.

The object oriented architectural clarity and standard java language support provided the key motivation for using the JiST/SWANS tool to simulate PML for WSN node localization. SWANS includes an implementation of the open systems interconnection (OSI) model for the physical, data link, network, transport and application layers and so provides a complete WSN simulation framework capable of modeling the real-world scenarios. The simulation testbed for PML using JiST was constructed as follows.

WSNs nodes were defined as independent objects associated with application, routing, networking, medium access control (MAC) and radio entities and were deployed in a physical environment represented by a field entity. All nodes were created with the same configuration with the anchor nodes being designated. To create a faithful WSN representation, typical IEEE 802.11b signal parameters were used, namely a radio frequency of 2.4GHz, transmit signal energy of 15 dBm, receiver signal threshold of -91dBm and bandwidth of 1MHz. The simulator also modeled the free-space path loss and fading. The complete set of parameters is listed in Table VI.

Using SWANS a multihop localization using RSS measurements has been developed employing multihop propagation techniques similar to Distance Vector routing. Each node maintains a table of anchor nodes and their range estimations by summing up multihop range estimations to the anchor. The nodes exchange *Hello Packets* to exchange the anchor table with neighboring nodes at 1 second interval. The receiving nodes compute the range to the sender and updates its anchor table from the received information. If there is already an entry for an anchor it updates the range only if it is smaller than the current entry.

The multihop distance estimation itself introduces additional error other than the RSS range estimation error as it approximates the range of an anchor by the minimum multihop distance to that anchor. Hence, multihop range estimations always give an over-estimation of the range and the minimum of all multihop distances are always chosen for a specific anchor.

Each of the regular nodes estimates its location from the anchor nodes and their measured ranges at 3 seconds interval. Following observation 1, the anchor node selection process in algorithm 1 has been developed to form pair of nodes that maximize the pair-wise equivalence of the RSS parameter, so PML operates in a totally distributed manner with nodes independently computing their location without incurring any central communications overhead.

The performance of the proposed technique is simulated using a random deployment of 200 nodes as shown in figure 6a. The interconnection diagram as the connections are made using freespace propagation model is shown in figure 6b. The variation of the RSS ranging error is achieved by manipulating the environmental path loss exponent n. The simulation is run on the same configuration of figure 6 for the period of 60 seconds with simulation preparation runtime of 6 seconds after which routing table becomes stable and statistics is collected.

The localization performance under various conditions are now described as follows.

A. Localization Performance under Ideal Simple Path Loss Model

Firstly, the impact of simple path loss model on localization is analyzed with the path loss exponent n of (4) being used and the corresponding performances of the triangulation and PML approaches displayed in figure 7. The key evaluation metric for localization is the estimation error extent compared to the ranging error. In figure 7 anchor percentage is varied while localization accuracy is plotted as the line graph with RSS range estimation error displayed in the shaded area.

It is apparent from figure 7 that PML depicted by diamond tagged solid line, provides a consistently better solution than the triangulation approach. RSS error indicates the error presence in the basic signal strength to range calculation and hence

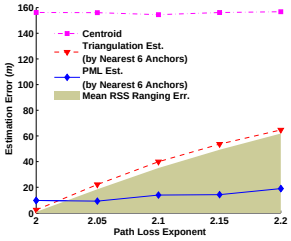

(a) 5% Anchor density.

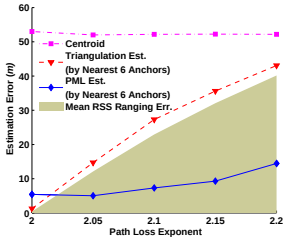

(b) 10% Anchor density.

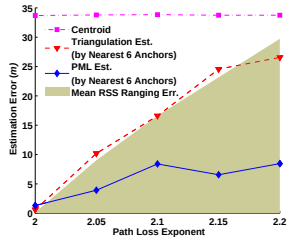

(c) 15% Anchor density.

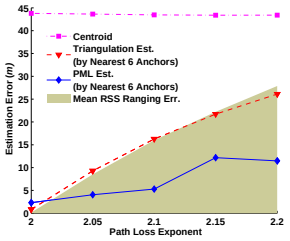

(d) 20% Anchor density.

Fig. 7: Performance comparison between Triangulation, PML and Centroid localization for 200 uniformly distributed WSNs nodes in a $500m \times 500m$ field for varying anchor densities using simple path loss model.

shown as shaded region in the chart. A clear trend is observed that for increasing RSS range estimation error the localization error also increases. The centroid approach provides nearly constant estimation error for all node densities as it does not employ range measurement and applies the mean of the anchor node positions around the source.

When n increases from 2 to 2.2 in (4), the net effects are an overall increase in RSS error. For $n = 2$, the error is nearly zero when the simple path loss model is observed, while for $n = 2.2$ the error is $\approx 30 - 45m$ which corresponds to measurement noise of nearly $50 - 75\%$ of the average communication range (hop distance) of $60m$. For the same value of n, the RSS error decreases with increasing anchor node percentages though the difference between 15% to 20% anchor node is very small as expected due to the presence of all nearest anchors within the single hop distance for increasing anchor percentages.

The PML performance degrades more gracefully than ranging error and most of the time PML is able to achieve better estimate than the average ranging error while triangulation performance follows the similar trend as of ranging error. With increasing anchor percentages triangulation performance improves as the ranging error decreases and for 20% it shows to perform better than the ranging error. The PML always performs much better than the ranging error and particularly for higher ranging error it shows independence to anchor percentages. It suggests that better ranging technique can improve the performance other than increasing the number of anchor nodes for WSNs localizations.

The centroid approach provides an upper limit on the estimation error and it is evident from the graphs that PML is able to estimate locations better than the average RSS error presence in the range estimation and thus improving the localization under noisy conditions significantly than usual triangulation. Triangulation shows to perform marginally better for average range error less than $0.5m$ as shown for environmental attenuation coefficient of 2.0. For all higher error conditions PML performs consistently better.

B. Localization Performance under Different Fading Models

The robustness of the PML is analyzed by the simulation of multipath fading channels following Rayleigh and Ricean fading models [27]. The former is typically applied to describe the statistical nature of the received envelope of a flat fading signal for Non Line of Sight (NLOS) scenarios, while for LOS conditions where a dominant component is present; the latter distribution is used [27]. The Rayleigh and Rician noise component at any instant as measured by signal strength can vary widely and so some filtering is necessary in order to limit its impact. For this experiment a 200 Hz sampling frequency is assumed with the noise averaged over this sampling interval.

The effect of multipath signal interference using Rayleigh fading distributions is presented figure 8. The results show that the impact of fading is minimized and PML consistently gives better results than the triangulation approach.

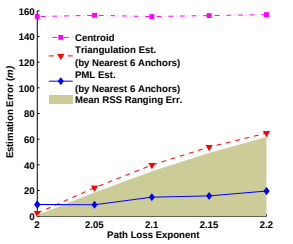

(a) 5% Anchor density.

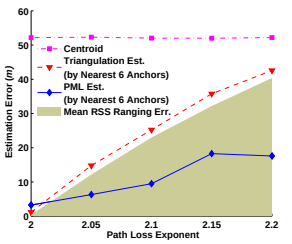

(b) 10% Anchor density.

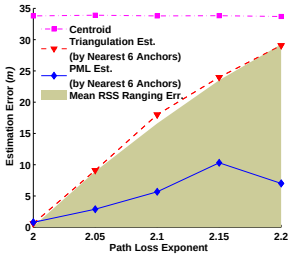

(c) 15% Anchor density.

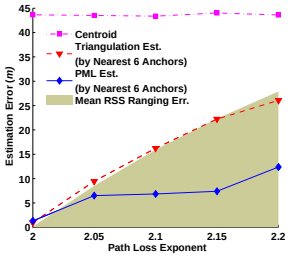

(d) 20% Anchor density.

Fig. 8: Performance comparison between Triangulation, PML and Centroid localization for 200 uniformly distributed WSNs nodes in a $500m \times 500m$ field for varying anchor densities using Rayleigh fading model.

The urban LOS signal interference effect is modelled using Rician fading distributions with one dominant signal and other multipath components. The performance results for this model are presented in figure 9.

In comparison with the simple path loss model results, it is evident that no significant difference in results are observed for different fading models. It is due to the cause that noise is averaged over 1 second interval as well as due to the

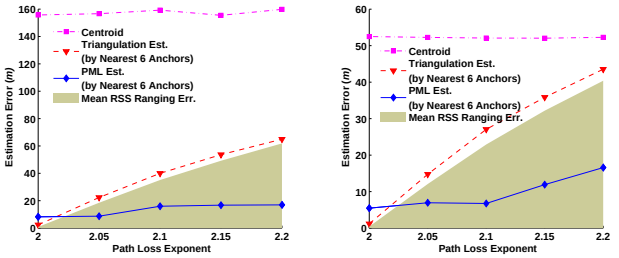

(a) 5% Anchor density. (b) 10% Anchor density.

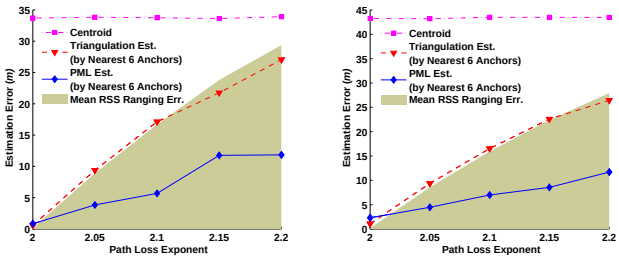

(c) 15% Anchor density. (d) 20% Anchor density.

Fig. 9: Performance comparison between Triangulation, PML and Centroid localization for 200 uniformly distributed WSNs nodes in a $500m \times 500m$ field for varying anchor densities using rician fading model.

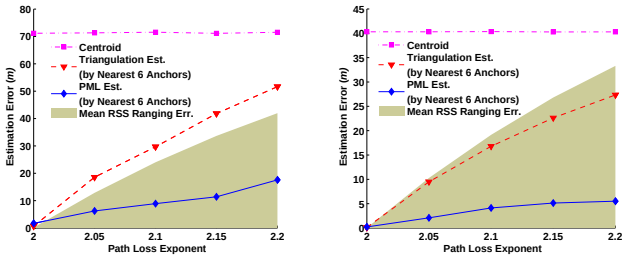

(a) 400 Nodes. (b) 600 Nodes.

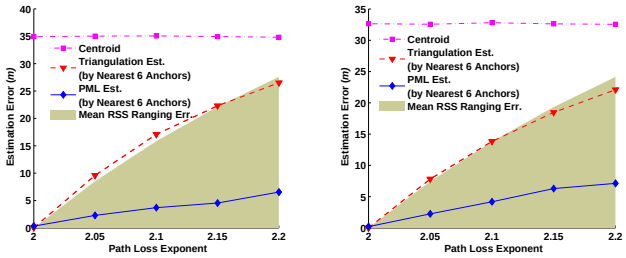

(c) 800 Nodes. (d) 1000 Nodes.

Fig. 10: Performance comparison between Triangulation, PML and Centroid localization for uniformly distributed WSNs nodes in a $500m \times 500m$ field for varying node densitieds with five percent anchor presence.

selection of nearest 6 anchors that are minimally affected by propagation noise. However, it validates the superiority of PML over triangulation under realistic propagation models suggesting its applicability in real life scenarios over existing approaches.

C. Localization Performance for Varying Node Densities

All the previous models were based upon the same node deployment scenario. In Figure 10 the performance for different uniform node deployments is presented with 5% anchor node presence. The results for other node densities follow a similar trend and validate the extendability of PML under different node densities and deployment scenarios with achieved localization accuracy within the close proximity to the RSS errors. Moreover, it validates that the proposed technique is able to support a very low anchor densities as the number of sensors increases.

D. The impact of Radio Irregularities

All the previous simulations were performed using spherical radio propagation model which is not quite realistic propagation model. The Radio Irregularity Model (RIM) proposed by [38] is shown to be a good model for incorporation into simulation tools. The RIM has been implemented into JiST for anisotropic adjustment of freespace path loss in different directions. The degree of irregularity parameter of the model is set at 0.01812 which is shown to be the most practical value for RIM [38]. In Figure 11 the comparative results for multi-hop localizations for different values of path loss exponent n

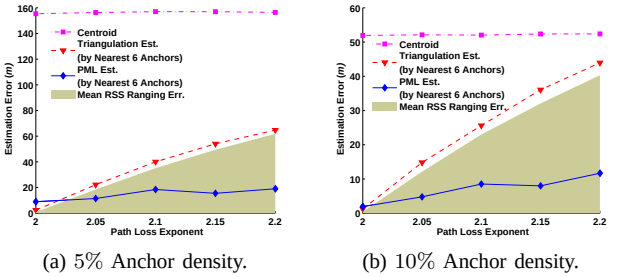

(a) 5% Anchor density. (b) 10% Anchor density.

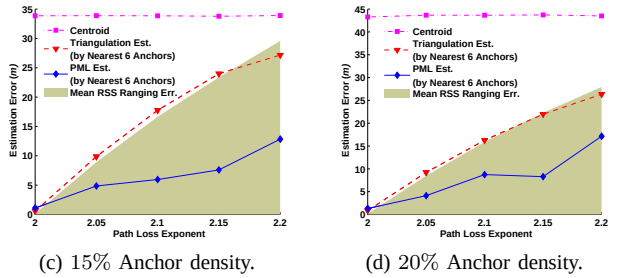

(c) 15% Anchor density. (d) 20% Anchor density.

Fig. 11: Performance comparison between Triangulation, PML and Centroid localization for varying anchor node densities with radio irregularity modelling that takes account of anisotropic radio propagation along different directions.

using RIM are shown which endorses the superiority of PML localization under irregular radio propagation.

JiST provided a realistic simulation environment for evaluation of localization performances under different RF conditions and propagation models. However, simulation results are always questionable as simulations are performed in a controlled environment while in practical cases there are many unknown parameters affecting the outcome. Hence a practical validation of the proposed approach is performed which is now described.

(a) Outdoor configuration with 10 motes. A single mote and its wooden platform is shown in the inset image.

(b) Indoor configuration with 10 motes. Motes are placed on top the cubicle separators as shown.

Fig. 12: Images of indoor and outdoor experimental setup for localization using 10 motes.

VII. Practical Test-bed Results

An experimental WSNs testbed is created for the practical evaluation of the proposed approach. Ten Moteiv [1] Tmote sky WSNs motes are used for the experiment. Eight motes are designated as anchor nodes, one is designated as unknown node and moved in different places for its localization and the last one is connected to a laptop for result aggregation. The motes are placed in the same orientation so that directional propagation issues can be evident by the placement of test mode in different positions. Every node maintains a table of neighbouring anchor nodes and their estimated ranges along with the sequence number of the packet from which the range is updated. Every node emits a beacon packet broadcasting its position (if it is an anchor itself), neighboring anchor positions, and estimated ranges every 5 seconds. The receiving node estimates range to the sender from the signal strength and updates its neighbor table for the sender. Anchor node ranges for the received neighbor table are augmented by current hop distance and that the motes neighbor table entries corresponding to relevant anchor are updated if the current range estimate from received packet is smaller or equal to already found range. Received packets and range updates are tracked by a packet sequence number so that only fresh range estimates are kept in the neighbor table. Triangulation and PML approaches employing nearest 6 anchors according to the received signal strength are compared [32]. The node to be localized is moved in different places and RSS data is collected for a period of three minutes for each placement. The localization is performed realtime on the mote as well as the signal strength data is sent to the base station for offline evaluation and verification of the data with obtained results.

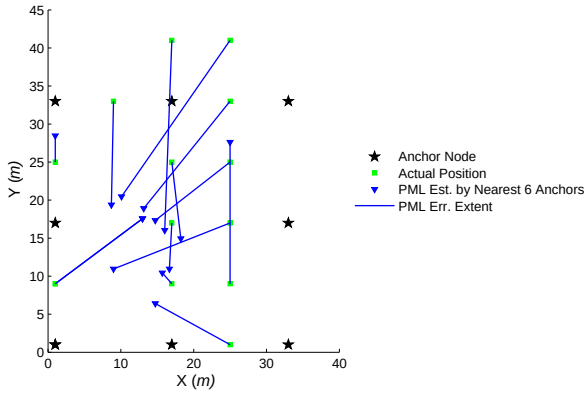

Fig. 13: Experimental setup and PML Performance for outdoor localization.

The experiment is performed in three different setups: *a*) outdoor open field configuration, *b*) indoor single room setup where each node is able to communicate with every other node and *c*) indoor setup extending to three adjacent rooms where some anchors are not within direct communication range of the others. Figure 12 shows the indoor and outdoor experimental photographs. The anchor node deployment schema and localization performances employing PML for the three environments are shown in figures 13, 14 and 15 respectively.

TABLE II: Outdoor Experimental Results for Triangulation and PML Estimations.

#	Original Position	Mean RSS Ranging Err.	Triang. Est. Err.	PML (Sing. Ref.) Err.	PML (Eq. Noise) Err.	PML (LOP Refine.) Err.
	(m)	(m)	(m)	(m)	(m)	(m)
1	(1, 9)	16.07	1010.16	1460.70	18.88	14.72
2	(1, 25)	8.57	1304.94	16.42	14.96	3.45
3	(9, 33)	9.80	1031.79	15.78	15.41	13.63
4	(17, 9)	7.86	1055.40	8.99	9.48	1.94
5	(17, 17)	13.14	790.02	59.22	3.17	6.06
6	(17, 25)	10.47	839.54	9.60	8.95	10.14
7	(17, 41)	10.05	1409.52	18.06	17.59	24.99
8	(25, 1)	11.52	1180.80	25.48	20.06	11.61
9	(25, 9)	8.00	697.57	49.88	7.90	18.61
10	(25, 17)	12.95	383.70	11.81	11.57	17.11
11	(25, 25)	11.21	1357.60	13.73	11.90	12.82
12	(25, 33)	11.04	1286.28	22.53	14.98	18.42
13	(25, 41)	13.85	1132.79	33.78	23.95	25.39

The triangulation approach produces large error for practical

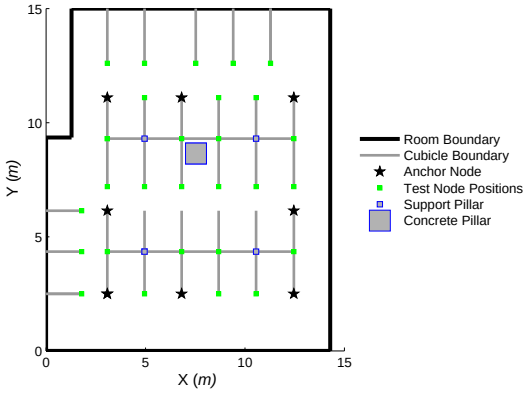

(a) Deployment scheme.

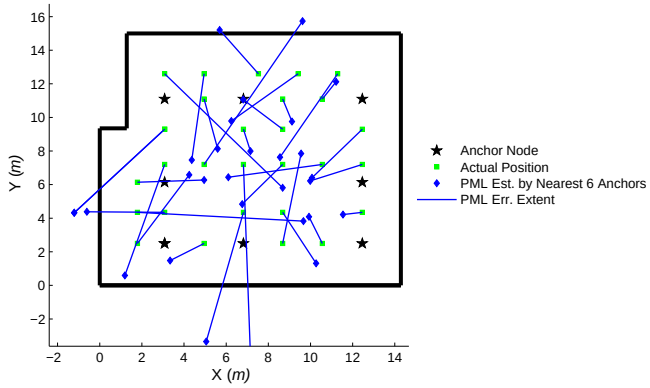

(b) Estimation results with error extent.

Fig. 14: Performance comparison between localization methods for test deployment of 10 motes in a single indoor room.

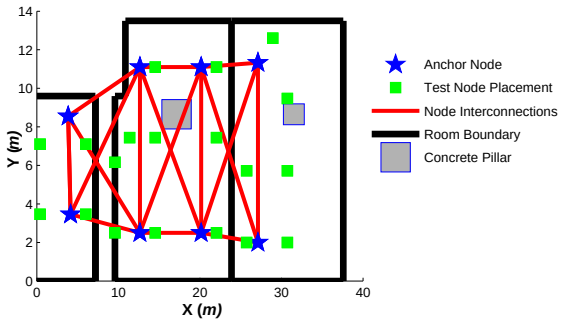

(a) Deployment scheme.

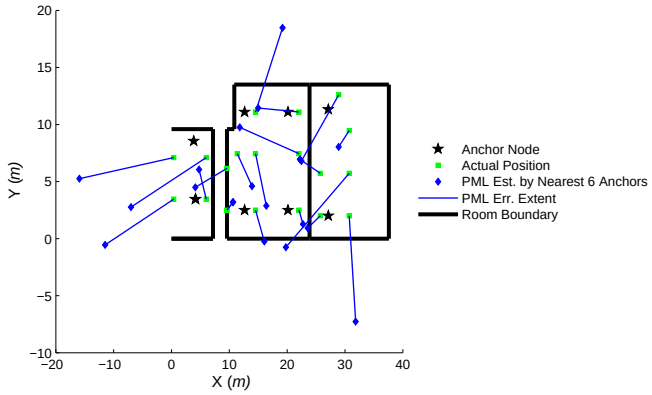

(b) Estimation results with error extent.

Fig. 15: Performance comparison between localization methods for test deployment of 10 motes in three adjacent indoor rooms.

results mainly due to the cause that error that is evident in practical environment is not uniform in all directions. Moreover, single path loss exponent $n = 2.0$ is used for all three cases which is another source of error in the range estimation. Due to the huge error margin for triangulation approach the performance for outdoor, indoor single room and indoor three rooms are presented in Tables II, III and IV respectively. As RSS based range measurement error is one of the fundamental criteria for assessment of localization performance these are presented by average of the RSS ranging error from contributing anchors alongwith triangulation and PML performances.

It is evident from tables II, III and IV that simulation results are rather conservative than the practical improvement by PML. As exemplified by simulations that under large margin of noise the PML performs increasingly better and hence the improved performance is quite commensurate with simulations.

The results highlight an important aspect of the basic assumption of equal range noise. For most of the cases PML approaches show large improvement over basic triangulation while for some cases PML (Single Ref. Anchor) and PML (Equal Noise Param.) shows degradation in estimation compared to triangulation. These are the cases when the presumed conditions are not fulfilled by the selected anchor pairs. Another important finding is that these degenerate cases are only evident for sources placed on the boundary of the region while the anchors appearing only one side of the node are used for localization. Hence, for a sufficiently dense deployment when anchor pairs can be chosen from alternate sides of the node such degradations can be avoided.

PML by LOP refinement process is however free from these glitches as it is consistent and always gives better estimation than triangulation. The practical setup is able to give clear validation of the proposed formulation for its adoption in real-life localization instead of basic triangulation that is the basis of most localization approaches till now.

Summarizing, PML is an improvement over triangulation-based localization in that it considers noisy measurement conditions in its formulation. The comparative results presented unequivocally endorse the potential of this new strategy for real time location estimation and tracking performance, with it being especially generic for a wide diversity of communication-based applications.

VIII. Conclusion

This paper has presented an analytical approach to source localization in Wireless Sensor Networks (WSNs) under noisy conditions. The paired measurement localization (PML) algo-

TABLE III: Indoor Single Room Experimental Results for Triangulation and PML Estimations

#	Original Position	Mean RSS Ranging Err.	Triang. Est. Err.	PML (Sing. Ref.) Err.	PML (Eq. Noise) Err.	PML (LOP Refine.) Err.
	(m)	(m)	(m)	(m)	(m)	(m)
1	(1.79, 2.5)	2.61	145.56	26.74	6.26	4.76
2	(1.79, 4.35)	1.93	136.31	7.85	5.85	7.89
3	(1.79, 6.14)	3.67	175.64	6.83	5.63	3.16
4	(3.08, 4.35)	2.35	83.12	38.41	5.21	3.69
5	(3.08, 9.3)	33.11	18.77	240.96	133.69	6.57
6	(3.08, 7.2)	66.57	14.85	791.98	1268.40	6.87
7	(3.08, 12.6)	3.59	133.11	8.71	7.22	8.80
8	(4.95, 2.5)	1.91	21.66	7.91	4.71	1.91
9	(4.95, 7.2)	4.10	229.51	9.99	3.69	4.73
10	(4.95, 11.1)	3.82	138.05	545.31	6.12	3.04
11	(4.95, 12.6)	1.66	91.77	6.77	6.12	5.17
12	(6.82, 4.35)	3.74	98.47	2.83	1.28	7.90
13	(6.82, 7.2)	2.47	147.17	1.45	1.03	12.67
14	(6.82, 9.3)	1.43	71.57	1.10	1.09	1.35
15	(7.53, 12.6)	1.55	88.41	16.49	10.61	3.19
16	(8.68, 2.5)	2.10	116.36	4.58	4.42	5.42
17	(8.68, 4.35)	1.35	207.34	2.72	2.88	3.42
18	(8.68, 7.2)	6.07	95.13	4.97	3.84	3.04
19	(8.68, 9.3)	1.26	180.10	12.43	1.88	2.57
20	(8.68, 11.1)	1.38	79.37	3.15	3.03	1.42
21	(9.41, 12.6)	2.07	166.15	5.82	4.75	4.24
22	(10.56, 2.5)	2.17	116.08	3.05	0.68	1.71
23	(10.56, 7.2)	3.76	80.71	0.67	2.95	4.52
24	(10.56, 11.1)	6.12	303.30	10.71	7.66	1.21
25	(11.29, 12.6)	2.60	174.45	5.26	6.07	5.68
26	(12.46, 7.2)	2.49	216.05	3.78	4.00	2.66
27	(12.46, 4.35)	4.77	135.77	22.91	18.45	0.93
28	(12.46, 9.3)	3.01	98.58	1.88	5.24	3.75

TABLE IV: Indoor Experimental Results Extending to Three Adjacent Rooms for Triangulation and PML Estimations

#	Original Position	Mean RSS Ranging Err.	Triang. Est. Err.	PML (Sing. Ref.) Err.	PML (Eq. Noise) Err.	PML (LOP Refine.) Err.
	(m)	(m)	(m)	(m)	(m)	(m)
1	(0.4, 3.46)	27.27	197.46	55.51	78.70	12.53
2	(0.4, 7.1)	22.85	356.49	113.39	51.89	16.42
3	(6, 3.46)	10.05	84.45	11.14	31.51	2.87
4	(6, 7.1)	12.28	88.15	62.48	27.38	13.72
5	(9.59, 2.5)	10.19	259.64	28.15	13.96	1.25
6	(9.59, 6.16)	12.57	149.06	710.70	5.67	5.73
7	(11.38, 7.44)	2.96	343.04	6.03	7.32	3.81
8	(14.53, 2.5)	4.11	226.39	6.69	2.98	3.14
9	(14.53, 7.44)	5.11	632.43	8.02	12.64	4.93
10	(14.53, 11.1)	9.75	687.19	1.50	1.90	8.74
11	(22.04, 11.1)	9.95	489.91	61.07	15.83	7.06
12	(22.04, 7.44)	17.98	364.79	22.62	1.44	10.48
13	(22.04, 2.5)	2.62	408.70	6.46	8.51	1.41
14	(25.73, 2)	9.50	789.21	19.45	16.15	2.44
15	(25.73, 5.72)	16.09	786.47	23.35	11.06	3.73
16	(28.93, 12.6)	9.52	1040.31	11.82	11.47	8.68
17	(30.73, 2)	6.55	501.23	0.83	8.66	9.34
18	(30.73, 5.72)	7.60	672.20	11.62	8.82	12.72
19	(30.73, 9.47)	7.56	706.02	5.30	4.90	2.32

rithm is underpinned by a mathematical framework following the hyperbolic locus of position under noisy conditions. Solution of the hyperbolic formulation is provided by three alternative approaches. The applicability of PML in real-world scenarios is justified by simulation and practical testbed results. PML is formulated for noisy conditions and proven to be particularly effective for received signal strength based range measurements, which are very important as they require either little or no additional hardware and are easily adapted to miniature WSNs devices. Comparative localization results for PML and the traditional Triangulation method confirm the fundamental argument that it consistently provides superior estimation performance with lower errors under realistic noisy conditions. Moreover, since PML is an analytical approach, it is computationally efficient and could help minimize data transmission between nodes once the anchor node selection process is completed. Another implication of the proposed PML is that it is an enhancement over basic triangulation with the cost of additional measurements and hence could be utilized in GPS receivers to minimize the adverse affect of timing asynchrony.

ACKNOWLEDGMENT

The authors would like to thank Professor Laurence Dooley for his suggestions and comments for the improvement of this paper.

REFERENCES

[1] Moteiv tmote sky wireless sensor mote. http://www.sentilla.com, 2008.

[2] P. Bahl and V. Padmanabhan. Radar: An in-building rf-based user location and tracking system. In *INFOCOM*, volume 2, pages 775–784, March 2000.

[3] Rimon Barr, Zygmund J. Haas, and R. V. Renesse. Jist: an efficient approach to simulation using virtual machines. *J. of Software: Practice and Experience*, 35 (6):539–576, February 2005.

[4] N. Bulusu, J. Heidemann, and D. Estrin. Gps-less low-cost outdoor localization for very small devices. *IEEE Personal Communications*, pages 28–34, October 2000.

[5] J. J. Caffery. A new approach to the geometry of toa location. In *52nd Vehicular Technology Conference*, 2000.

[6] S. Capkun, M. Hamdi, and J. P. Hubaux. Gps-free positioning in mobile ad-hoc networks. *Cluster Computing*, 5(2):157–167, 2002.

[7] Y.T. Chan and K.C. Ho. A simple and effificient estimator for hyperbolic location. *IEEE Transactions on Signal Processing*, 42:1905–1915, 1994.

[8] Joe C. Chen, Ralph E. Hudson, and Kung yao. Maximum-likelihood source localization and unknown sensor location estimation for wideband signals in the near-field. *IEEE Transactions on Signal Processing*, 50 (8):1843–1854, AUG 2002.

[9] K. K. Chintalapudi, A. Dhariwal, R. Govindan, and G. Sukhatme. Ad-hoc localization using ranging and sectoring. In *INFOCOM*, March 2004.

[10] L. Doherty, K. S. J. Pister, and L. E. Ghauri. Convex position estimation in wireless sensor networks. In *INFOCOM*, Anchorage, AK, April 2001.

[11] D. Estrin, L. Girod, G. Pottie, and M. Srivastava. Instrumenting the world with wireless sensor networks. In *International Conference on Acoustics, Speech, and*

Signal Processing (ICASSP 2001), pages 2675–2678, Salt Lake City, Utah, May 2001.

[12] D. Fox, W. Burgard, H. Kruppa, and S. Thrun. A probabilistic approach to collaborative multi-robot localization. *Springer J. Autonomous Robots*, 8:325–344, 2000.

[13] W. H. Foy. Position-location solutions by taylor-series estimation. *IEEE Trans. Aerosp. Electron. Syst.*, 12:187–194, march 1976.

[14] B. Friedlander. A passive localization algorithm and its accuracy analysis. *IEEE J. Ocean. Eng.*, 12:234–245, january 1987.

[15] T. He, C. Huang, B. M. Blum, J. A. Stankovic, and T. Abdelzaher. Range-free localization schemes for large scale sensor networks. In *MOBICOM*, pages 81–95, 2003.

[16] J. Hightower, C. Vakili, G. Borriello, and R. Want. Design and calibration of the spoton ad-hoc location sensing system. Technical report, 2001. URL http://citeseer.ist.psu.edu/hightower01design.html.

[17] L. Hu and D. Evans. Localization for mobile sensor networks. In *MOBICOM*, pages 45–57, 2004.

[18] Y. Hu, A. Perrig, and D. Johnson. Packet leashes: A defence against wormhole attacks in wireless ad hoc networks. In *INFOCOM*, April 2003.

[19] Koen Langendoen and N. Reijers. Distributed localization in wireless sensor networks: A quantitative comparison. *Elsevier J. of Computer Networks*, 43:499–518, 2003.

[20] J. Li, J. Jannotti, D.S.J. DeCouto, D.R. Karger, and R. Morris. A scalable location service for geographic ad-hoc routing. In *MOBICOM*, August 2000.

[21] J. Li, Y. Zhang, and F. Zhao. Robust distributed node localization with error management. In *MOBIHOC*, 2006.

[22] D. Moore, J. Leonard, D. Rus, and S. Teller. Robust distributed network localization with noisy range measurement. In *Proc. of the 2nd international conference on Embedded networked sensor systems (SenSys)*, 2004.

[23] D. Niculescu and B. Nath. Ad-hoc positioning system. 2001.

[24] N. Patwari, J. N. Ash, S. Kyperountas, A. O. Hero III, R. L. Moses, and N. S. Correal. Locating the nodes: Cooperative localization in wireless sensor networks. *IEEE Signal Processing Magazine*, July 2005.

[25] G. J. Pottie and W. J. Kaiser. Wireless integrated network sensors. *Communications of the ACM*, 43:51–58, 2000.

[26] N. B. Priyantha, A. Chakraborty, and H. Balakrishnan. The cricket location-support system. In *MOBICOM*, August 2000.

[27] T. S. Rappaport. *Wireless Communication - Principles and Practice*. Prentice-Hall, Inc., New Jersey, USA, 1996.

[28] S. Roumeliotis and G. Bekey. Collective localization: a distributed kalman filter approach. In *Proc. of ICRA*, pages 2958–2965, May 1999.

[29] Chris Savarese, Koen Langendoen, and Jan Rabaey. Robust positioning algorithms for distributed ad-hoc wireless sensor networks. In *Proc. USENIX Tech. Ann. Conf.*, pages 317–328, 2002.

[30] A. Savvides, C. Han, and M. Srivastava. Dynamic fine-grained localization in ad-hoc networks of sensors. In *MOBICOM*, JULY 2001.

[31] A Savvides, W.L.Garber, R.L. Moses, and M. Srivastava. An analysis of error inducing parameters in multihop sensor node localization. *IEEE Transactions on Mobile Computing*, 4(6), 2005.

[32] A. H. Sayed, A. Tarighat, and N. Khajehnouri. Network-based wireless location: Challenges faced in developing techniques for accurate wireless location information. *IEEE Signal Processing Magazine*, July 2005.

[33] X. Sheng and Y. H. Hu. Maximum likelihood multiple-source localization using acoustic energy measurements with wireless sensor networks. *IEEE Transactions on Signal Processing*, 53:44–53, January 2005.

[34] S. Slijepcevic, S. Megerian, and M. Potkonjak. Location errors in wireless embedded sensor networks: Sources, models and effects on applications. *ACM SIGMOBILE Mobile Computing and Comm. Review*, 6(3):67–78, 2002.

[35] J. O. Smith and J. S. Abel. Closed-form least-squares source location estimation from range-difference measurements. *IEEE Trans. Acoust., Speech, Signal Process.*, 35:1661–1669, december 1987.

[36] D. J. Torrieri. Statistical theory of passive location systems. *IEEE Trans. Aerosp. Electron. Syst.*, 20:183–197, 1984.

[37] K. Whitehouse and D. Culler. Calibration as a parameter estimation problem in sensor networks. In *Proc. of ACM Workshop on Sensor Networks and Applications*, 2002.

[38] G. Zhou, Tian He, S. Krishnamurthy, and J. A. Stankovic. Models and solutions for radio irregularity in wireless sensor networks. *ACM Trans. On Sensor Networks*, 2 (2):221–262, 2006.

[39] Y. Zu, J. Heidemann, and D. Estrin. Geography-informed energy conservation for ad hoc routing. In *MOBICOM*, JULY 2001.